

Microfabricated sensors for the measurement of electromagnetic fields in biological tissues

James Monberg and Albert K. Henning

Thayer School of Engineering, Dartmouth College, Hanover NH 03755-8000

ABSTRACT

Public awareness of the risks of exposure to electromagnetic radiation has grown over the past ten years. The effects of power lines on human and animal health have drawn particular attention. Some longitudinal studies of cancer rates near power lines show a significant correlation, while others show a null result. The studies have suffered from inadequate sensors for the measurement of electromagnetic radiation *in vivo*.

In this work, we describe the design, construction, and testing of electrically passive, microfabricated single-pole antennas and coils. These sensors will be used *in vivo* to study the effects of electromagnetic radiation on animals. Our testing to date has been limited to *in vitro* studies of the magnetic field probes. Magnetic field pickup coils were fabricated with up to 100 turns, over a length of up to 1000 μm . Measurements were carried out with the sensors in air, and in water of various saline concentrations. Magnetic fields were applied using a Helmholtz coil. Both dc and ac fields were applied. The results indicate that small-area measurements of electromagnetic fields *in vitro* can be made successfully, provided adequate shielding and amplification are used.

Keywords: magnetic field sensor, electric field sensor, micro-solenoid, micro-fabricated electromagnetic field sensor, *in vitro* and *in vivo* EMF sensor, EMF microprobe.

1. INTRODUCTION

Electromagnetic fields (EMFs) were first reported as biologically harmful in 1979¹. Subsequent studies have examined the biological effects of EMFs. No conclusive findings have been made as to the exact mechanism of biological harm, nor that harm exists irrefutably². The measurement of EMFs has been a weak experimental link. Although researchers are split on whether the induced electrical field (**E**-field) or magnetic field (**B**-field) is of chief biophysical interest, there has been little work in the design and construction of probes for measuring *in vivo* EMFs, especially **B**-fields. Attempts have been made with miniature **E**-field probes³⁻⁶. Most designs revolve around the use of silver chloride wire and hypodermic needles.

The construction of microscale **B**-field probes requires a technology beyond the designs currently in use for **E**-field measurement. Micromachine technology such as MUMPs (Multi-User Microelectromechanical Machine Processes)⁷ has enabled construction of sensors and actuators microns in size. This study examines the viability of using micromachine technology to construct *in vivo* **B**-field probes. Probe designs are founded upon an extensive review of the relevant epidemiological work in EMF research, and an understanding of the probe design physics, and the capabilities and limitations of micromachine technology.

2. THE BIOLOGICAL EFFECTS OF EMFs

The effects of EMFs on biological tissues have been reviewed in detail⁸. In this section, we highlight the salient features.

2.1. The Biophysics of Electric and Magnetic Fields

A time varying electric field \mathbf{E} or magnetic field \mathbf{B} will exert a force \mathbf{F} on a charged particle, given by:

$$\mathbf{F} = q(\mathbf{E} + \mathbf{v} \times \mathbf{B}) \quad (1)$$

where q is the particle and \mathbf{v} is the velocity. The force effect of the \mathbf{E} -field on q is many orders of magnitude larger than the \mathbf{B} -field⁹. Many researchers therefore study only the \mathbf{E} -field. This conclusion assumes the fields act through a force mechanism without *a priori* proof that the transductive step between EMF exposure and biological harm involves physical force.

The relationship between the \mathbf{B} -field and induced \mathbf{E} -field is expressed formally by Faraday's law:

$$\frac{\partial \mathbf{B}}{\partial t} = -\nabla \times \mathbf{E} \quad (2)$$

The \mathbf{E} -field produced by a time varying but uniform magnetic field is given as:

$$\mathbf{E} = -\frac{S}{\lambda} \frac{\partial \mathbf{B}}{\partial t} \quad (3)$$

where λ is the path enclosing the surface area S . The most easily measured effect of this field would be the current density $\mathbf{J} = \sigma \mathbf{E}$ where σ is the conductivity of the tissue. Mathematical models of induced current density in the human body begin with this relation and develop further based on models of anatomical geometry. A common method¹⁰ models the human body as a uniformly conductive ellipsoid of revolution with the major axis, z , parallel to the long axis of the body. If a sinusoidal magnetic field with amplitude B_0 is incident along the z axis, then the peak amplitude of the induced current density in a plane described by the orthogonal x and y coordinate axes is given by:

$$J = \frac{2\pi B_0 \sigma}{a^2 + b^2} (b^4 x^2 + a^4 y^2)^{1/2} \quad (4)$$

where a and b are the semi-axes of the ellipsoid. The induced currents circulate in loops with a plane defined by the x and y coordinates (orthogonal to the z axis)¹¹. This model and ones quite similar to it are seen extensively in the literature^{9,11-13}. However, models can never fully take into account the wide and varied conductivities within the human body. Moreover the physical structure of organs, bones, muscles, and various connective tissues impact the propagation of \mathbf{B} - and \mathbf{E} -fields; whole-body models ignore these endogenous geometries. Of course Faraday's equation must apply inside the body, but the appropriate boundary conditions are probably most accurately applied to individual tissue systems such as organs rather than whole body systems.

Magnetic fields by themselves can only exert a force on ferromagnetic materials. This force is given by:

$$\mathbf{F} = \mathbf{m} \cdot \nabla \mathbf{B} \quad (5)$$

where \mathbf{m} is the dipole moment and $\nabla \mathbf{B}$ is the gradient of the magnetic flux density. Biological systems are capable of synthesizing small properties of magnetite Fe_3O_4 ⁹. Bees, pigeons, salmon, and some bacteria use these particles organized into strings roughly a micron in length to navigate in the earth's magnetic fields. These lifeforms are capable of sensing changes 10 μG changes in the earth's magnetic field, 60 times smaller than the average 60 Hz measured in Denver homes⁹. The recent discovery of remnant magnetization in the

human brain¹⁴ could provide a mechanism for coupling weak **B**-fields to biological systems in a significant way⁹. A mechanism wherein cell potentials are changed to affect the pressure receptor sensing mechanisms in nerve cells has been discussed¹⁵. A possible pressure of 0.4 N/m² applied to cell membranes is calculated due to coupling from a 1 mG field. This peak pressure is much larger than the radiation pressure of .0001 N/m² required to enhance or inhibit the firing of nerve fibers in the sciatic nerve of the frog¹⁵. Thus, the dipoles of strongly coupled magnetic particles have the potential to modify ion transport processes across cell membranes with applied B-fields as low as 1.0 mG⁹.

Other magnetic field effects have been proposed. Chemically reactive free radicals have been modeled as sensitive to 60 Hz radiation¹⁶. The 10 Hz cyclotron frequency of calcium ions¹⁷, crucial to cell membrane biochemistry, may be disrupted by **B**-fields¹⁸, and possibly explains observed changes in membrane transport phenomena¹⁹. This latter model has been criticized for mathematical flaws²⁰ and its biochemical assumptions²¹.

2.2. Characteristics and Pervasiveness of Ambient EMFs

It is necessary to know the magnitude of external fields, in order to design a probe sensitive to the resultant internal fields. Table 1 lists measured values for power sources typically encountered in society²²⁻²⁵.

Table 1. Magnetic and Electric Field Strengths Encountered in Society

Source	Magnetic		Electric	
	Typical	Maximum	Typical	Maximum
	(mG)		(V/m)	
High-tension lines	20-25	90	1000	7000
Electric railroad (13 kV, 60 Hz)	35	300	350	700
Electric railroad (11 kV, 25 Hz)	126	650	300	600
Transformer substation	15-25	---	---	---
Distribution lines (12 kV)	1-3	20	5-40	60
Secondary lines (240/120 V)	5-10	100-200	---	---
Pole-to-home	1	4	---	---
<i>Household 60 Hz sources:</i>				
Wiring	0.5-1	5-10	1-5	10
Microwave oven (30-300 cm distance)	0.1	7	---	---
Dishwasher (30-300 cm)	0.05	3	---	---
Hair dryer (3-30 cm)	6.6	1200	---	---
Can opener (3-30 cm)	47	6000	---	---
Blender (3-30 cm)	2	550	---	---
Shaver (3-30 cm)	6	1200	---	---

The natural exposure to magnetic and electric fields may far outweigh any man-made source²¹. The earth's magnetic field varies from about 300 mG at the equator to over 700 mG at the poles. However, this field source is time invariant. Other sources of high-magnitude time varying fields include cellular telephones and video display terminals. The focus of this work is, however, on low frequency (30-300 Hz) field sources.

2.3. Biological Harms of 60 Hz Electromagnetic Fields

Visual flickering due to magnetophosphenes occur when human subjects are exposed to either pulsed or sinusoidal fields at frequencies below 100 Hz and intensities as low as 100 mG²⁶. Magnetophosphenes are induced in the region of the retina. They cause additional neurochemical/electrical effects upon exposure to fields two orders of magnitude higher than those causing the visual changes alone²⁷.

Time varying magnetic fields induce electric fields in tissue. Current densities higher than 1 A/m² cause neural excitation and irreversible biological effects such as cardiac fibrillation^{11,28,29}. **B**-fields causing this magnitude of current are rarely encountered outside the laboratory. Natural current densities in humans range from 0.1-10 mA/m². Current densities above this range induced by magnetic fields effect the biochemistry and physiology of cells and organized tissues. These effects include: altered cell growth rate; decreased rate of cellular respiration; altered metabolism of carbohydrates; proteins, and nucleic acids;

effects on gene expression and genetic regulation of cell functions; teratological and developmental effects; morphological effects and tissue changes in animals (reversible); endocrine system alterations, including melatonin suppression in the pineal gland; altered hormonal responses of cells and tissues; altered immune response to antigenic stimulation; and nonspecific neurobehavioral effects^{1,10,11,30,31}.

Low frequency fields are not considered a direct carcinogen³². These fields may have some role as a pro-carcinogen or co-carcinogen where they either act as a precursor to cancer or in combination with another agent to cause cancer. EMFs have been clearly linked with cancer¹. An increased incidence of some types of cancer in populations exposed to higher power EMFs in a residential setting has been reported³³. Workers operating electrical machinery have high mortality due to central nervous system cancers³⁴. Increased incidence of brain tumors in electrical workers has been studied³⁵. Studies in Scandinavia found an increased incidence of leukemia and brain tumors^{36,37}.

Positive correlations in these studies sometimes indicate no more than a 5% incidence increase. This low increase indicates these fields affect the cellular level and increase the risk to certain types of cancer. The exact mechanism, or transductive step, between the fields and their effects on tissue is still the missing link.

Other important biological harms have been reviewed elsewhere⁸. Together with the cancer-related effects, they show that the biological effects of EMFs cannot yet be firmly described, indicating the need for new means to measure EMFs *in vivo*.

3. MEASUREMENT OF EMFs

There are two methods for measurement of biologically relevant EMFs. The first measures local internal **E**-fields induced by external **B**-fields *per* Faraday's law. The second measures gross **B**-field exposure externally. There are important drawbacks for both methods, as surveyed below.

Measurement of induced **E**-fields was pioneered in the 1980s^{3,4}. **E**-field probes consisting of fine filaments of silver-chloride wire and some associated connection circuitry were constructed. These probes were very thin but almost 2 cm long, making them inappropriate for *in vivo* applications. Life-sized, or quarter-scale¹⁵, styrofoam mannequins, or saline, approximated the conductivity of the human body. Three electrodes have been fitted into the tip of a hypodermic needle^{5,6}. Problems with these techniques include: the human body does not have a constant conductivity; the internal geometry of the body is highly varied (membranes can affect field propagation) such that the local **B**-field (and hence the **E**-field) may not be in good agreement with the *in vitro* model; hypodermic needles make a "hole" that fills with blood, and the resultant conductivity of the surrounding tissue can yield errors in measurement as high as 78% (for the case of a blood-filled hole in muscle tissue)³⁸.

The measurement of *in vitro* or *in vivo* **B**-fields using miniature probes is conspicuously absent from the literature. The relative complexity of **B**-field vs. **E**-field probes may explain this absence, along with the disposition of EMF researchers to focus on local **E**-fields. The technology of measuring **B**-fields centers on fairly large meters usually "worn" by the individual. Several such meters have been designed³⁹⁻⁴¹. However, they are only useful in measuring *external* EMF exposure. No studies have correlated external exposure with internal, or cellular level, **B**-fields.

4. MICROPROBE DESIGN AND FABRICATION

With this background in mind, we determined to design **B**-field and **E**-field probes using microfabrication technology, with a primary focus on **B**-field probes. At 60 Hz, and given the proximities alluded to in Table 1, our problem was essentially the detection of near-field radiation, lending itself to a lumped circuit element solution, rather than a transmission line or antenna solution. The **E**-field detectors could be simple linear probes. The **B**-field inductors would need to incorporate coils to measure induced **B**-field strength. According to Faraday's Law, the electromotive force v induced in a stationary circuit is equal to the negative rate of increase of magnetic flux ϕ linking the circuit:

$$v = - \frac{d\phi}{dt} \quad (6)$$

If the ambient **B**-field is given by:

$$\mathbf{B} = B_0 \sin(\omega t) \hat{\mathbf{z}} \quad (7)$$

then magnetic flux linking N turns of probe coil with radius b:

$$\phi_{\text{one turn}} = \oint_S \mathbf{B} \cdot d\hat{\mathbf{s}} \quad (8)$$

$$\phi_{N \text{ turns}} = N \pi b^2 B_0 \sin(\omega t) \quad (9)$$

The emf induced is then:

$$v = N \pi b^2 B_0 \omega \cos(\omega t) \quad (10)$$

The factor πb^2 can be replaced by the coil cross-sectional area for non-symmetric coils. The emf must be sufficient for sensing. Also, ultimately, we seek a probe which measures field contributions along three perpendicular axes, in order to calculate the general field magnitude.

The design criteria for a **B**-Field probe are: small size - $\leq 1\text{mm} \times 1\text{mm}$; sensitive, able to measure fields as small as 1 mG at 60 Hz; accurate - measure 3D gain within 5% after calibration; biocompatible - bionutral material construction, stable geometry. The design criteria for an **E**-Field probe are: small in size - $\leq 1\text{mm} \times 1\text{mm}$; sensitive, able to measure currents in the picoamp range; accurate - measure current within 5% after calibration; biocompatible - bionutral material construction, stable geometry.

Microprobes were constructed using the MUMPs technology (Multi-User Microelectromechanical systems Process)⁷. It is a three-layer polysilicon surface micromachining process designed to provide as much flexibility as is consistent with process stability. Polysilicon is used as the structural material, phosphosilicate glass (PSG) as the sacrificial material, and silicon nitride for electrical isolation from the substrate. Polysilicon is highly biocompatible^{42,43}.

Sensors were designed using the microfabrication mask layout tool L-Edit (Tanner, Inc., Los Angeles, CA). A number of parameters were investigated. **E**-field microprobe lengths were varied from 10 to 1000 μm , and constructed from degenerately doped polysilicon. These probes were either bare conductors over their entire length, or shielded coaxially over part of their length. Substrate ground planes were included on half the devices. Provisions were made for the probes to be insulated with either silicon dioxide (PSG), if the devices were left without subsequent processing; or air, if this oxide were removed using a global hydrofluoric acid (HF) release etch as a last step. Probes were oriented in both the x- and y-directions.

B-field microprobe lengths were varied from roughly 20 to 1000 μm . The number of coils in the probes was varied from 10 to 250. Probes were laid out in both x- and y-directions. (Subsequently, we determined z-axis microprobes could be fashioned simultaneously from spiraling coils, in the same manner that inductors were fabricated in Josephson junction microelectronic circuits. This result would yield full three-axis field measurements using a planar fabrication technology. Folded structures⁴⁴ to obtain z-axis measurements are also under consideration.) While the lateral portion of the coil cross-section (a rectangle) could be controlled, the vertical dimension was set at only a few micrometers by the MUMPs process. In order to

increase this vertical dimension to its largest possible value, a ‘false wax’ technique using the second polysilicon layer was utilized. This technique was implemented using the large bar with the ‘handhold’ at one end, seen in Figure 3. After the oxide is removed from this device using HF, the bar is withdrawn, leaving behind a relatively large cross-sectional area probe. Without the bar, the third polysilicon layer will be much closer to the substrate, reducing the sensitivity of the microprobe.

Initial designs were submitted for fabrication in March, 1995 and returned from MCNC in May, 1995. Figure 1 shows the global mask design generated using L-Edit. Figure 2 shows a scanning electron microscope (SEM) photograph of an E-field microprobe, while Figure 3 shows its B-field probe counterpart. Micrographs were obtained using a Zeiss DSM-962 SEM.

Our characterizations to date have concentrated on the B-field microprobes. We note, however, that the greatest challenge with the E-field probes may be the complete loss of any signal gain when the probes are connected with an external measuring device. Off-chip amplification (see below) may forestall this problem. On-chip amplification at the probe site⁴⁵, or amplification using the proposed MCNC flip-chip MUMPs technology add-on⁴⁶, are under consideration.

The initial devices returned from MCNC were fabricated using a design lacking contacts between the third polysilicon layer (the upper-level diagonals in Figure 3) and the first polysilicon layer. Upon release using HF, this top polysilicon layer floats free, destroying the structure’s utility. We attempted to make high frequency measurements on this faulty microprobe, but calculated the frequency necessary to shunt the capacitors at each first poly-third poly interface was far beyond our measurement capability. The corrected design was re-submitted to MCNC, and was received for testing in early August, 1995. At press time for these proceedings, characterization measurements on these microprobes had not begun.

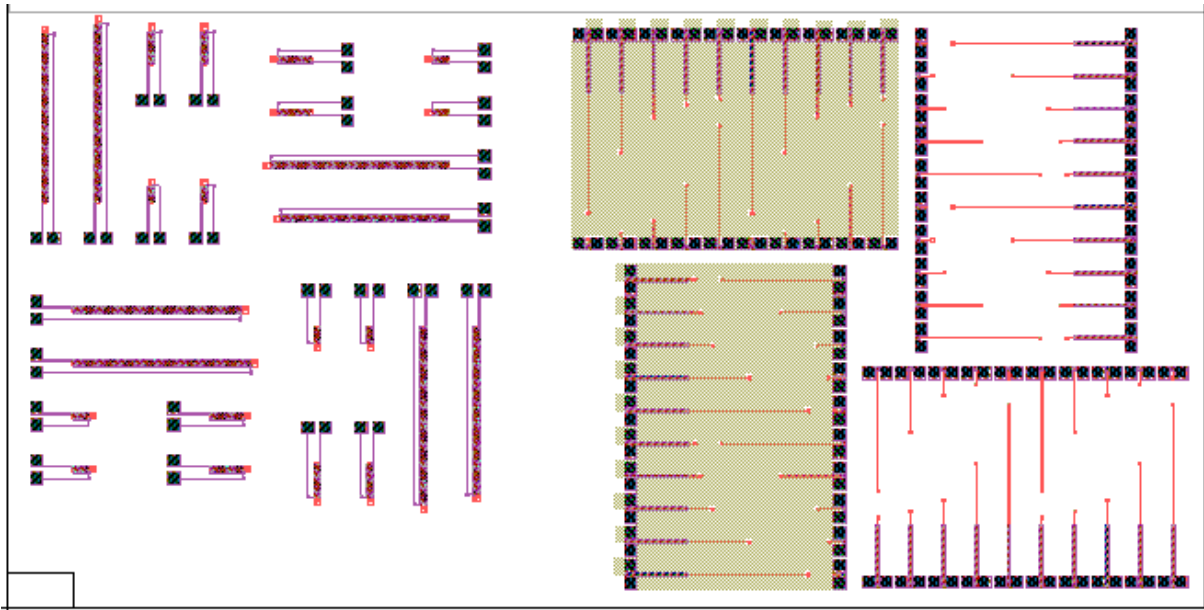


Figure 1: L-Edit mask design based on the MUMPs process. B-field probes are on the left; E-field probes are on the right.

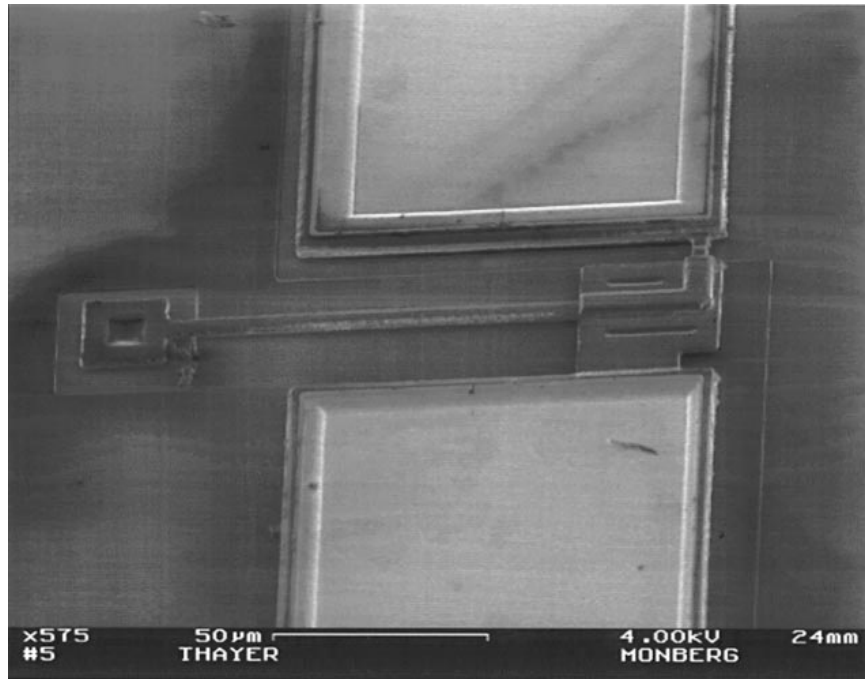


Figure 2: SEM of an E-field microprobe. The contact electrodes (square pads in the micrograph) are coated with gold. The length of the probe is 250 μm.

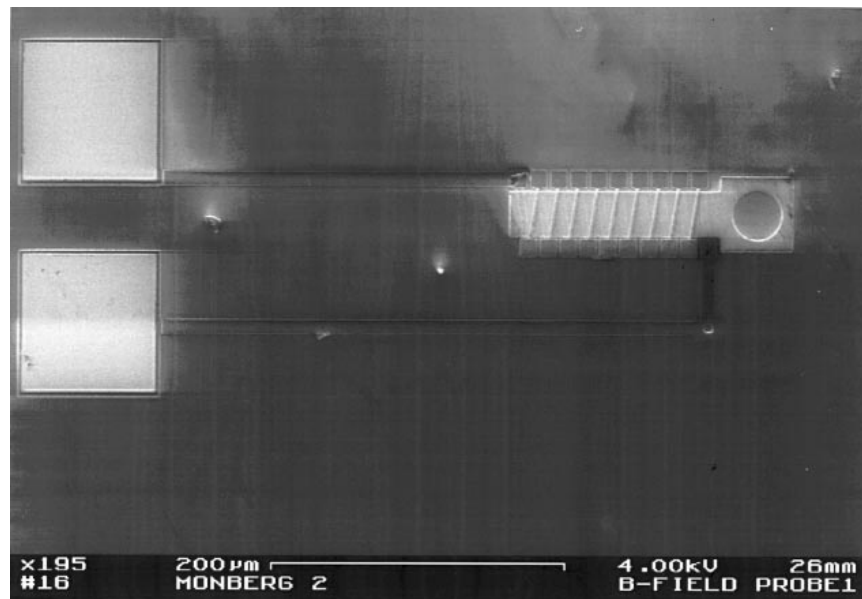


Figure 3: SEM of a B-field microprobe.

5. MACROSCALE MAGNETIC FIELD PROBES AND PROBE CALIBRATION

Macroscale probes were also designed and constructed. The intent was to prove the viability of the smaller designs through the use of scaling theory. If larger probes could output a sufficient signal when exposed to an appropriate **B**-field, then smaller probes should scale commensurately.

The macroscale probes were built with .012" varnished copper wire. The wire was wound around a steel rod .04" in diameter. The number of turns N was set at 15, 30, and 60. Initial attempts at mechanized winding (to

ensure uniform loop size and juxtaposition) using commercially available wire wrappers proved ineffective in that the remaining lead was not long enough. The coils were carefully hand wound to the specified number of turns with several inches of lead remaining. The tips of the leads were exposed with fine sanding using 800 grit paper.

The testing apparatus had two main components: first, the **B**-field generating apparatus; and second the measurement apparatus and associated hardware and software. The **B**-fields were generated with a small set of Helmholtz coils. These coils were not calibrated spatially; we assume the field is constant in a region within 10% of the midpoint between the two coils. A non-ferromagnetic mounting platform was machined out of acrylic to hold the probes (both macro and micro) within the constant **B**-field region. The platform also has provisions for modifying the orientation of the probe in the field. The Helmholtz coils were driven with an AC signal provided by a Wavetek function generator. The signal input to the coils was verified on a HP54501A Digital Oscilloscope. Figure 4a shows a schematic of this apparatus. Measurements were done inside a fully shielded (aluminum) box.

Since specifications of the Helmholtz coils were unknown (i.e. number of turns), an empirical calibration was completed using an MGH-1 milligaussmeter. The gaussmeter probe was affixed on the acrylic probe platform in the same manner used for the test probes. The Helmholtz coils were then driven with a 60 Hz signal. The amplitude of the signal was varied and the V_{rms} was measured at each variance. The **B**-field was also measured in milligauss for each variance. The measured **B**-field was then compared to the input V_{rms} at each point. A plot of the calibration curve is shown in Figure 5. Linear regression analysis indicates strong linearity (r-squared is very close to unity) in the data. An equation for this calibration curve was developed which yields the resultant **B**-field for any given input V_{rms} .

The probe signal output was measured on a HP54501A digital oscilloscope. The output signal was measured for frequency and V_{rms} . Given the sensitivity of the digital oscilloscope, an operational amplifier circuit was designed to amplify the output signal and reject line noise. The topology of the circuit is shown in Figure 4b. An OP-07 op-amp was used that has a common mode rejection ratio (CMRR) on the order of 10^7 . The CMRR is defined as $\text{CMRR} = A_d / A_c$, where A_c and A_d are the gains of common mode and difference mode signals, respectively. The use of the difference mode allows the rejection of line noise. This amplified signal was clearly readable on the oscilloscope for 60Hz inputs.

Each macroprobe was affixed to the same position on the acrylic platform, and evaluated at seven input points corresponding to 10-40 mG applied **B**-field strengths with 5 mG increments. The actual applied **B**-field was determined using the calibration curve. The signal output was measured on the digital oscilloscope. The results are shown in Figure 6. The error bars represent standard deviations from several measurements on each macroprobe.

Considering Equation 10, the slope of the signal should increase as N increases. We observe this result in Figure 6. Furthermore, scaling theory suggests our microprobes will also provide appropriate signals using our measurement system. Assuming (worst-case) the microprobe vertical dimension is $1.5 \mu\text{m}$, and the lateral dimension is $10 \mu\text{m}$, then the microprobe will generate a signal $1/625$ of the macroprobe signal for a given **B**-field. While this signal is measurable in our system, it represents a lower bound. Microprobes with larger vertical and lateral dimensions, and with more coils, have already been constructed which will enhance the signal output.

Although other frequencies were not investigated in this work, it is reasonable to assume these probes will also be useful to measure 50 Hz fields, of significance in Europe.

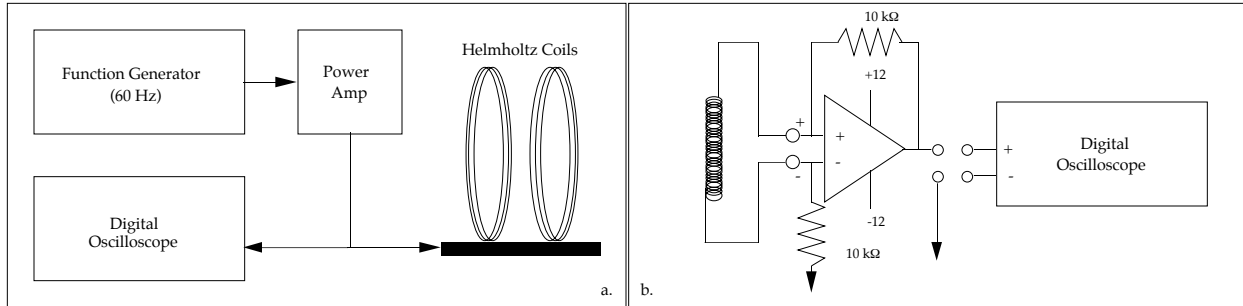


Figure 4. a. Block diagram of the test and measurement system; b. Circuit diagram of the sensor amplifier.

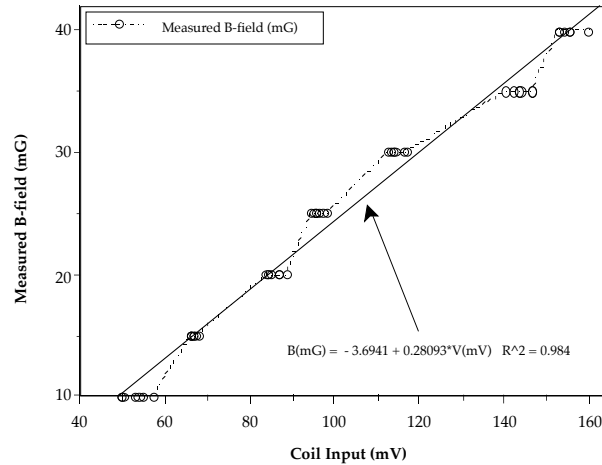


Figure 5. Calibration curve for the Helmholtz coil.

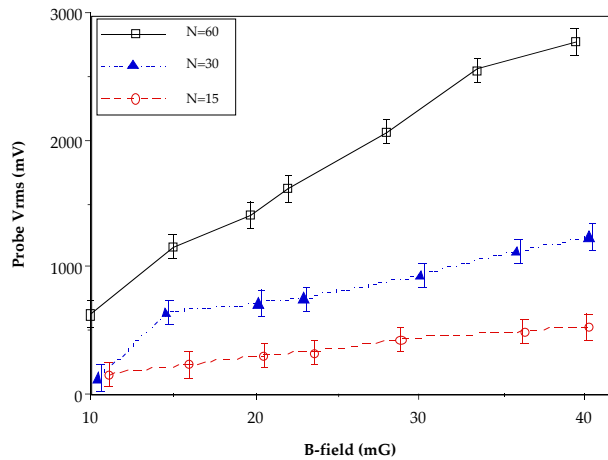


Figure 6. Measured output from the macroprobe vs. applied B-field strength.

6. CONCLUSIONS

Electromagnetic fields in the ELF range have some biological effects. Their exact in role in cancer remains to be seen but the overwhelming epidemiological evidence of empirical reactions to ELF fields cannot be ignored. The precise mechanism or transductive step of biological reaction has not been clearly established but may be better understood when researchers can better characterize endogenous electric and magnetic fields. There is no probe currently capable of measuring such fields. There is reason to believe that the measurement of internal magnetic fields may provide the most accurate insight as to what electric fields

may be induced internally.

In this study, microprobes were designed and constructed for measuring *in vivo* EMFs. Both micro- and macro-scale magnetic field probes were fabricated, and their responses to appropriate magnetic field strengths characterized. The results show these probes meet the specifications necessary for viable use *in vivo*.

Further work will involve testing the second generation microprobes in the current testing apparatus, followed by *in vitro* tests using tissue phantoms to approximate the permeability of tissue. The third phase will involve development and testing of three dimensional microprobes, as well as consideration of the practicality/necessity of inclusion of the operational amplifier directly on the microprobe. The fourth phase will examine *in vivo* use of the device, through the use of humane laboratory animal testing.

7. ACKNOWLEDGEMENTS

The authors acknowledge the following, with gratitude: the staff of the Microelectronics Center of North Carolina, particularly Allen Cowen, David Koester, and Karen Markus, for assistance with MUMPs; Christopher Dietrich of the Thayer School of Engineering, for assistance with the amplifier circuit design; Christopher Levey and Chia-lun Tsai of Thayer School, for assistance with release etching of the finished structures; William Doyle of the Dartmouth Physics Department, for discussions on near- and far-field radiation probes; Ralph Gibson of the Dartmouth Physics Department, for loan of the Helmholtz coils and gaussmeter; and Charles Daghlian of the Dartmouth Electron Microscopy Facility for assistance with SEM photos.

8. REFERENCES

1. N. Wertheimer and E. Leeper, "Electrical wiring configurations and childhood cancer." *Amer. J. Epidem.* **109**, pp. 273-284 (1979).
2. W.R. Bennett, "Cancer and power lines." *Phys. Today* **47**, pp. 23-29 (1994).
3. W.T. Kaune, W.C. Forsythe, "Current densities measured in human models exposed to 60-Hz electric fields." *Bioelectromag.* **6**, pp. 13-32 (1985).
4. W.T. Kaune, W.C. Forsythe, "Current densities induced in swine and rat models by power-frequency electric fields." *Bioelectromag.* **9**, pp. 1-24 (1988).
5. D.L. Miller, "Miniature-Probe measurements of electric fields and currents in rat and human models." *Bioelectromag.* **12**, pp. 157-171 (1991).
6. D.L. Miller, "Magnetically induced electric fields measured in rats and compared to homogeneous rat model." In *Electricity and Magnetism in Biology* M. Blank, Ed. (San Francisco Press, San Francisco, 1993) pp. 533-565.
7. D.A. Koester, R. Mahadevan, K.W. Markus, *Multi-User MEMS Process (MUMPs): Introduction and Design Rules* (MCNC, ed. rev. 3, October 1994).
8. J. C. Monberg, *Micromachined Probes for Detection and Measurement of Extremely Low Frequency Electromagnetic Fields*. Senior Honors Thesis (Thayer School of Engineering, Dartmouth College, Hanover, NH, June 1995).
9. F.S. Barnes, "Some engineering models for interactions of electric and magnetic fields with biological systems." *Bioelectromag. Supp.* **1**, pp. 67-85 (1992).
10. T.S. Tenforde, "Biological interactions of extremely-low-frequency electric and magnetic fields." *Bioelectrochem. Bioenerget.* **25**, pp. 1-17 (1991).
11. T.S. Tenforde, "Biological Interactions and potential health effects of extremely-low-frequency magnetic fields from power lines and other common sources." *Annu. Rev. Pub. Health* **13**, pp. 173-96 (1992).
12. M. Miskasian, A.R. Sheppard, D. Krause, M.E. Frazier, D.L. Miller, "Biological, physical, and electrical parameters for in vivo studies with ELF magnetic and electric fields: a primer." *Bioelectromag. Supp.* **2**, pp. 1-73 (1993).
13. W. Xi, M.A. Stuchly, G.P. Om, "Induced electric currents in models of man and rodents from 60 Hz magnetic fields." *IEEE Trans. Biomed. Eng.* **41**:11, pp. 1019-1023 (1994).
14. J.L. Kirschvink, *Personal Communication*. Presentation at the First World Congress for Electricity and Magnetism in Biology and Medicine. June, 1992.
15. R.T. Mihran, F.S. Barnes, H. Wachtel, "Temporally-specific modifications of myelinated axon excitability in vitro following a single ultrasonic pulse." *Ultrasound in Med. and Biol.* **16**, pp. 297-309 (1990).
16. K. McLauchlan, "Are environmental magnetic fields dangerous?" *Phys. World*, January, pp. 41-45 (1992).
17. W.R. Adey, "Biological Effects of Electromagnetic Fields." *J. Biocell. Biochem.* **51**, pp. 410-416 (1993).
18. V.V. Lednev, "Possible mechanism for the influence of weak magnetic fields on biological systems." *Bioelectromag.* **12**, pp. 71-75 (1991).
19. J. Walleczek, "Electromagnetic field effects on cell of the immune system: the role of calcium signalling." *FASEB Journal* **6**, pp. 3177-3185 (1992).
20. R.K. Adair, "Criticism of Lednev's mechanism for the influence of weak magnetic fields on biological systems." *Bioelectromag.* **13**, pp. 231-235 (1992).
21. W.R.J. Bennet, *Health and Low Frequency Electromagnetic Fields* (Yale U. Press, New Haven, 1994).
22. D.L. Mader and S.B. Peralta, "Residential Exposure to 60-Hz magnetic fields for appliances." *Bioelectromag.* **13**, pp. 287-301 (1992).
24. L.J. Dlogosz, T. Byers, J. Vena, M. Zielesny, "Ambient 60-Hz Magnetic Flux Density in an Urban Neighborhood." *Bioelectromag.* **10**, pp. 187-196 (1989).

25. D.A. Savitz, T. Ohya, D.P. Loomis, R.S. Senior, T.D. Bracken, R.L. Howard, "Correlations among indices of electric and magnetic field exposures in electric field utility workers." *Bioelectromag.* **15**, pp. 193-204 (1994).
26. M.A. d'Arsonval, "Dispositifs pour la mesure des courants alternatifs toutes frequences." *C.R. Soc. Biol. (Paris)* **3**:100 (Ser.), pp. 450-451 (1896).
27. J. Silny, "The influence threshold of a time-varying magnetic field in the human organism." In *Biological Effects of Static and Extremely Low Frequency Magnetic Fields* J. H. Bernhardt, Ed. (MMV Medizin Verlag, München, 1986), pp. 105-112.
28. J. Bernhardt, "The direct influence of electromagnetic fields on nerve and muscle cells of man within the frequency range of 1 Hz to 30 MHz." *Radiat. Environ. Biophys.* **16**, pp. 309-323 (1979).
29. J.P. Reilly, "Peripheral nerve stimulation by induced electric currents: exposure to time varying magnetic fields." *Med. Biol. Eng. Comp.* **27**, pp. 101-110 (1989).
30. T.S. Tenforde, "Interaction of ELF magnetic fields with living matter." In *Handbook of Biological Effects of Electromagnetic Radiation* E. B. C. Polk, Ed. (CRC, Boca Raton, 1986), pp. 197-225.
31. T.S. Tenforde, "Biological interactions and human health effects of extremely low frequency magnetic fields." In *Extremely Low Frequency Electromagnetic Fields: The question of cancer* R. G. S. B.W. Wilson, L.E. Anderson, Ed. (Batelle Press, Columbus, Ohio, 1990), pp. 291-315.
32. M.R. Cook, C. Graham, H.D. Cohen, M.M. Gerkovich, "A replication study on human exposure to 60 Hz fields: effects on neurobehavioral measures." *Bioelectromag.* **13**, pp. 261-285 (1992).
33. D.A. Savitz, H. Wachtel, F.A. Barnes, E.M. John, J.G. Tvrdik, "Case-control study of childhood cancer and exposure to 60-Hz magnetic fields." *Am. J. Epidem.* **324**, pp. 727-733 (1988).
34. J. Raloff, "Physicists offer reassurances on EMF (a report on the March 1995 APS meeting)." *Science News* **147**:20, p. 308 (1995).
34. T.F. Mancuso, "Epidemiological study of tumors of the central nervous system in Ohio." *Ann. NY Acad. Sci.* **381**, pp. 17-39 (1982).
35. T.L. Thomas, P.D. Stolley, A. Stemhagen, E.T.H. Fontham, M.L. Bleecker, P.A. Sterart, R.N. Hoover, "Brain tumour mortality risk among wiht electrical and electronic jobs." *J. Nat'l. Cancer Inst* **79**, pp. 233-237 (1987).
36. S. Tornqvist, B. Knave, A. Ahlbom, T. Persson, "Incidence of leukemia and brain tumors in some electrical occupations." *Brit. J. Ind. Med.* **48**, pp. 245-292 (1991).
37. T. Tynes, A. Andersen, F. Langmark, "Incidence of cancer in Norwegian workers potentially exposed to electromagnetic fields." *Amer. J. Epidem.* **136**, pp. 81-88 (1992).
38. D.L. Miller, "Conductivity differences distort probe measurements of magnetically induced electric fields." *Bioelectromag.* **15**, pp. 483-487 (1994).
39. P. Héroux, "A dosimeter for assessment of exposures to ELF fields." *Bioelectromag.* **12**, pp. 241-257 (1991).
40. M.J. Hagmann and T.M. Babij, "Noninvasive measurement of current in the human body for electromagnetic dosimetry." *IEEE Trans. Biomed. Eng.* **40**:5, pp. 418-423 (1993).
41. W.T. Kaune, J.C. Niple, M.J. Liu, J.M. Silva, "Small integrating meter for assessing long-term exposure to magnetic fields." *Bioelectromag.* **13**, pp. 413-427 (1992).
42. S. Schmidt, K. Horch, R. Normann, "Biocompatibility of silicon-based electrode arrays implanted in feline cortical tissue." *J. Biomed. Mat. Res.* **11**, pp. 1393-1399 (1993).
43. D. Fedida, S. Sethi, B.J.M. Mulder, H.E.D.J. Keurs Tur, "An ultracompliant glass microelectrode for intracellular recording." *Amer. J. Physiology* **258**, pp. 164-170 (1990).
44. K.S.J. Pister, *Hinged Polysilicon Structures with Integrated CMOS Thin Film Transistors*. Ph.D. dissertation (U. California, Berkeley, CA, 1992).
45. G.T.A. Kovacs, C.W. Storment, M. Halks-Miller, C.R. Belczynski, C.C.D. Santana, E.R. Lewis, N.I. Maluf, "Silicon-substrate microelectrode arrays for parallel recording of neural activity in peripheral and cranial nerves." *IEEE Trans. Biomed. Eng.* **41**, pp. 567-577 (1994).
46. K. Markus, Microelectronics Center of North Carolina, Research Triangle Park, NC. *Personal Communication*, August 3, 1995. Also available using the Internet at: <http://www.mcnc.org>.